

TABLE 1 Diversity Performances of Dual-Band IFAs with Neutralization Line

	IFAs in Free Space		IFAs + Head		IFAs + Head + Hand	
	0.826	2.6	0.826	2.6	0.826	2.6
Frequency (GHz)	0.826	2.6	0.826	2.6	0.826	2.6
ρ	0.21	0.04	0.24	0.1	0.25	0.1
MEG ₁ (dB)	-2.6	-3.2	-6.3	-5.6	-7.2	-7.8
MEG ₂ (dB)	-2.6	-3.1	-5.7	-5.9	-7	-7.2

pattern diversity performances. The lower the correlation, the better is the antenna diversity performances [9]. The MEG is defined as the ratio between the mean received power of antennas over the random route and the total mean incident power [10]. When each antenna receives the same quantity of power, the MEG ratio between antennas is equal to one.

The calculated envelope correlation and MEGs of the two IFAs from simulated radiation patterns in the central frequency of each band are presented in Table 1.

In free space, a low correlation is observed in the two bands ($\rho_e < 0.21$) thanks to a low coupling between antennas ($|S_{21}| < -10$ dB) and polarization diversity naturally achieved by the orthogonal positions of IFAs. The envelope correlation increases slightly in presence of hand and head. It achieves 0.25. It can be seen that the ratio of MEG₁, determined at Port 1, over MEG₂, determined at Port 2 is almost equal to 1 for free space for the two frequencies, which satisfies equal contribution of the two antennas to receive the same quantity of power. Absorption of power in the head and distortion of the radiation pattern induce lower MEG's for both antennas, as shown in Table 1. The presence of hand decreases more MEGs. In addition, an unbalance receive power by each antenna is observed. This difference is caused by the different positions of each antenna relative to the head and hand. Despite the presence of human body, good diversity performances are obtained with $\rho_e < 0.5$ and MEG₁/MEG₂ is around 1 which provides high diversity capabilities. The study of dual-band diversity antenna integrated into mobile phone near human body has been also done. The same behaviors have been observed.

6. CONCLUSION

Integration of multiple antennas in LTE handheld devices, operating at low frequencies such as 790 MHz is a real challenge. The proposed dual-band diversity antenna is addresses to resolve this issue. Indeed, the proposed structure can operate in the two LTE bands: 790–826 MHz and 2.5–2.69 GHz. Thanks to neutralization line between antennas, the mutual coupling is reduced to -10 dB in the two bands. In addition, the first design can be integrated on a terminal such as a mini tablet, when the second is integrated into a mobile phone. Measurement results are in good agreement with simulated ones. Furthermore, the two IFAs still cover the desired bands with an acceptable radiation in presence of human body and satisfy the condition $\rho_e < 0.5$ and MEG₁/MEG₂ $\simeq 1$ in most of studied cases, which provides a good diversity. Therefore, proposed dual-band diversity antenna is suitable for MIMO multi-input multi-output systems.

ACKNOWLEDGMENT

The author would like to thank Dr. Anne Claire Lepage and Pr. Xavier Begaud from Institut Mines Telecom, Telecom Paris-Tech, CNRS, LTCI, Paris, France.

REFERENCES

1. A. Paulraj, D. Gore, R. Nabar, and H. Bölcskei, An overview of MIMO communications, A key to gigabit wireless, Proc IEEE 92 (2004), 198–218.
2. L. Hui, L.B. Kiong, and H. Sailing, Angle and polarization diversity in compact dual-antenna terminals with chassis excitation, In: General Assembly and Scientific Symposium, 2011, pp. 1–4.
3. L. Mouffok, A.C. Lepage, J. Sarrazin, and X. Begaud, Compact dual-band dual-polarized antenna for MIMO LTE applications, Int J Antennas Propag (2012), 1–10.
4. S. Cui, Y.Liu, W. Jiang, and S. Gong, Compact dual-band monopole antennas with high port isolation, Electron Lett 47 (2011), 579–580.
5. A. Diallo, C. Luxey, P. Le Thuc, R. Staraj, and G. Kossiavas, Study and reduction of the mutual coupling between two mobile phone PIFAs operating in the DCS1800 and UMTS bands, IEEE Trans Antennas Propag 154 (2006), 3063–3074.
6. K.L. Wong, H.J. Jiang, and T.W. Weng, Small-size planar LTE/WWAN antenna and antenna array formed by the same for tablet computer application, Microwave Opt Technol Lett 55 (2013), 1928–1934.
7. J.H. Lu and F.C. Tsai, Planar internal LTE/WWAN monopole antenna for tablet computer application, IEEE Trans Antennas Propag 61 (2013), 4358–4363.
8. W.T. Chen and H.R. Chuang, Numerical computation of human interaction with arbitrarily oriented superquadric loop antennas in personal communications, IEEE Trans Antennas Propag 46 (1998), 821–828.
9. R. Vaughan and J. Andersen, Antenna diversity in mobile communication, IEEE Trans Veh Technol 36 (1987), 149–172.
10. T. Taga, Analysis for mean effective gain of mobile antennas in land mobile radio environments, IEEE Trans Veh Technol 39 (1990), 117–131.

© 2014 Wiley Periodicals, Inc.

COMBINED-TYPE DUAL-WIDEBAND ANTENNA FOR 2G/3G/4G TABLET DEVICE

Li-Yu Chen and Kin-Lu Wong

Department of Electrical Engineering, National Sun Yat-sen University, Kaohsiung 80424, Taiwan; Corresponding author: wongkl@ema.ee.nsysu.edu.tw

Received 15 April 2014

ABSTRACT: A combined-type dual-wideband antenna with its lower wideband and higher widebands, respectively, contributed by two separate radiating portions thereof is presented. The two separate radiating portions (one low-band antenna and one high-band antenna) are easily combined into a compact structure for the 2G/3G/4G operation in the 698–960 and 1710–2690 MHz bands. In addition, for applications in the typical tablet device such as a tablet computer, the proposed antenna requires a very small ground clearance of 10×30 mm² for the 2G/3G/4G operation. The low-band antenna for the 698–960 MHz band is an inverted-F antenna, with its radiating arm coupled to the antenna's feeding strip through a first chip inductor and its shorting strip embedded with a second chip inductor. The high-band antenna for the 1710–2690 MHz band is a monopole antenna formed by connecting a simple strip to the feeding strip and enclosed by the low-band antenna so as to achieve a compact antenna structure. A simple matching circuit disposed on the device ground plane can, respectively, widen the bandwidth of the antenna's lower and higher bands. The proposed combined-type antenna can easily achieve dual-wideband operation with a small

Key words: mobile antennas; combined-type antennas; inverted-F antennas; tablet device antennas; small antennas; dual-wideband antennas

1. INTRODUCTION

The inverted-F antenna has been a promising antenna structure for the mobile device application [1,2]. For recent applications to cover the 2G/3G/4G operation in the 698–960 and 1710–2690 MHz bands, many promising internal antennas related to the inverted-F antenna structure have been reported. Some examples of the related antenna design can be seen in Refs. [3–13]. It is noted that to provide two wide operating bands with a decreased antenna size, multiple resonant modes are generally required to be excited in the higher wideband (1710–2690 MHz), such that a wide operating band of about 1 GHz in bandwidth can be formed. Some resonant modes in the higher band may also share the same resonant path with the resonant mode in the lower band (698–960 MHz). That is, the same resonant path is used to generate its fundamental mode in the lower band and its higher-order modes in the higher band. This will make the antenna’s lower and higher bands highly correlated. In this case, the tuning of the antenna’s low-band radiating portion for the desired low-band operation may also significantly affect the antenna’s high-band operation. Similarly, the tuning of the antenna’s high-band radiating portion for the desired high-band operation may also strongly affect the antenna’s lower-band operation. This will cause inconvenience or difficulties in fine adjusting the desired lower and higher bands for practical applications.

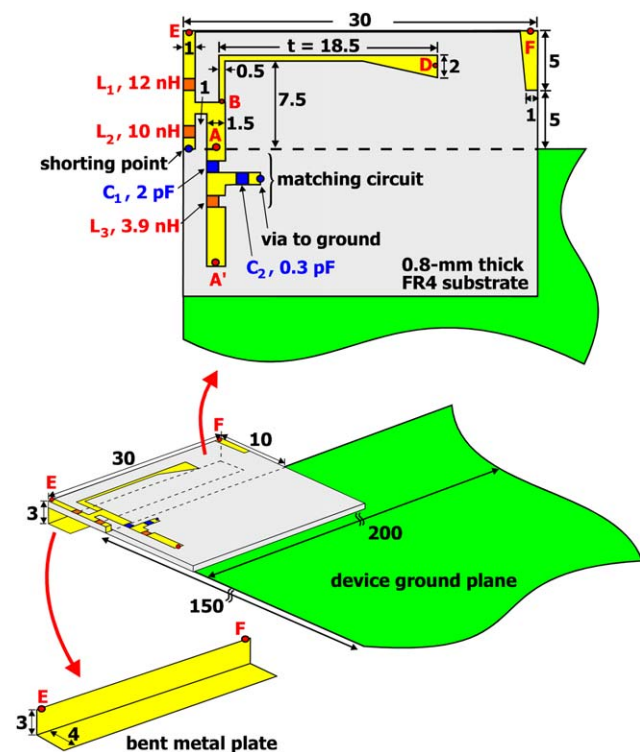


Figure 1 Geometry of the combined-type dual-wideband antenna for the 2G/3G/4G tablet device. [Color figure can be viewed in the online issue, which is available at wileyonlinelibrary.com]

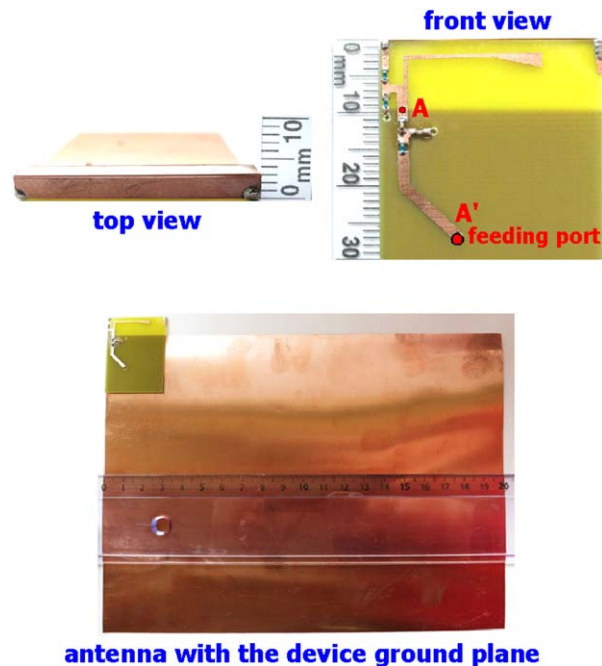


Figure 2 Photos of the fabricated antenna and the same with the device ground plane for the experimental testing. [Color figure can be viewed in the online issue, which is available at wileyonlinelibrary.com]

Hence, it motivates this study of using a combined-type antenna design to achieve the low-band and high-band operations for the internal 2G/3G/4G tablet device antenna. In the proposed combined-type antenna, the low-band and high-band radiating portions thereof are less correlated, and the low-band and high-band operations can generally be independently controlled by the low-band and high-band radiating portions. Furthermore, the two radiating portions can be combined into a compact structure, such that the antenna requires a small ground clearance in the mobile device. With attractive features of small size and easy fine adjusting the desired dual-wideband operation, the combined-type antenna will be attractive for practical mobile device applications.

In this article, a promising combined-type antenna with small size and dual-wideband operation for the 2G/3G/4G tablet device is demonstrated. The antenna’s lower and higher widebands are contributed by two separate radiating portions. The low-band radiating portion (denoted as the low-band antenna here) is an inverted-F antenna, wherein its radiating arm is coupled to the feeding strip through a first chip inductor and its shorting strip is embedded with a second chip inductor. The high-band radiating portion (denoted as the high-band antenna) is a monopole antenna formed by connecting a simple strip to the feeding strip and enclosed by the low-band antenna so as to achieve a compact antenna structure. The proposed antenna requires a very small ground clearance of $10 \times 30 \text{ mm}^2$ in a typical tablet computer. Note that very few of the reported 2G/3G/4G tablet device antennas can fit in a small ground clearance of less than $10 \times 40 \text{ mm}^2$ inside the tablet device [3–18].

The antenna also has a thin thickness of 3 mm only, which makes it attractive for modern slim tablet device or tablet computer applications. A simple matching circuit disposed on the device ground plane can, respectively, widen the bandwidth of the antenna’s lower and higher bands to cover the desired 698–960 and 1710–2690 MHz bands. In addition, owing to the embedded chip inductors in the low-band antenna, which

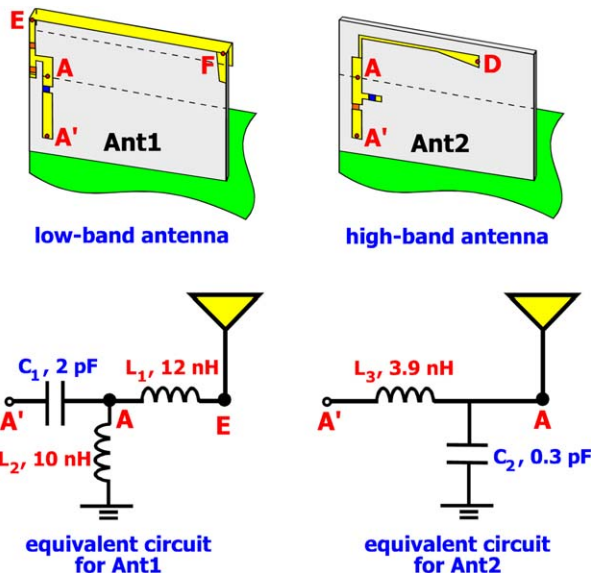


Figure 3 Structures of Ant1 (the low-band antenna) and Ant2 (the high-band antenna) and their equivalent circuit models. [Color figure can be viewed in the online issue, which is available at wileyonlinelibrary.com]

provide high inductive reactance for frequencies in the higher band and can function like an open circuit [19–21], the antenna's high-band operation can generally be independently controlled by the high-band antenna. This makes the proposed combined-type antenna easy in adjusting its desired lower and higher widebands for the 2G/3G/4G applications. Details of the proposed antenna are presented in the study.

2. PROPOSED ANTENNA

Figure 1 shows the geometry of the proposed combined-type dual-wideband antenna for the 2G/3G/4G tablet device. A photo of the fabricated antenna in this study is shown in Figure 2, wherein the fabricated antenna mounted along the top edge of the device ground plane of size $150 \times 200 \text{ mm}^2$ for the experimental study is also shown. The photo can make the proposed antenna more clearly for understanding. The experimental result will be presented and discussed in Section 4. Note that the selected dimension of the device ground plane is suitable for applications in the 9.7-inch tablet computer.

The proposed antenna can be decomposed into a low-band antenna and a high-band antenna as shown in Figure 3. The low-band and high-band antennas are denoted as Ant1 and Ant2 in the figure, and their equivalent circuit models are also shown for comparison. The low-band antenna is mainly an inverted-F antenna. The main radiating arm of the inverted-F antenna is the bent metal plate, which is connected to the feeding strip (section AB) through a chip inductor (L_1) of 12 nH. The inductor L_1 can lead to a decreased resonant length of the low-band antenna to generate a resonant mode at about 900 MHz [22–25]. The chip inductor (L_2) of 10 nH embedded in the shorting strip and the chip capacitor (C_1) of 2 pF in the matching circuit are formed as a high-pass matching circuit to greatly enhance the low-band bandwidth to cover the desired 698–960 MHz band.

When operated at higher frequencies in the desired higher band, the inductors L_1 and L_2 will provide high inductance to behave like an open circuit. In this case, the bent metal plate and the shorting strip can have very small effects on the antenna's high-band operation. In addition, the high-pass matching circuit

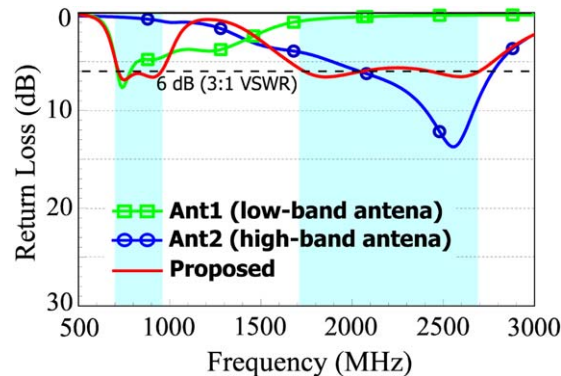


Figure 4 Simulated return loss for the proposed antenna, Ant1 (the low-band antenna), and Ant2 (the high-band antenna). Corresponding dimensions of the three antennas are the same. [Color figure can be viewed in the online issue, which is available at wileyonlinelibrary.com]

(L_2 and C_1) will also show small effects at high-band frequencies. Hence, in the desired higher band, the proposed antenna can be considered as the high-band antenna shown in Figure 3. The high-band antenna is a simple monopole antenna with a radiating strip (section AD) and a low-pass matching circuit formed by a parallel chip capacitor (C_2) and a series chip inductor (L_3). Tuning the length of section AD can adjust the excited resonant mode in the desired higher band while the low-pass matching circuit results in an additional resonance occurred near the excited resonant mode so as to greatly enhance the high-band bandwidth to cover the desired 1710–2690 MHz band.

Note that the low-band and high-band antennas can be combined in a compact configuration as shown in Figure 1 to occupy a small ground clearance of $10 \times 30 \text{ mm}^2$. The proposed antenna has a printed metal pattern on a 0.8-mm thick FR4 substrate and a bent metal plate cut from a 0.2-mm thick copper plate in the experiment. In this case, the total thickness of the proposed antenna is 3 mm only, which makes it promising for applications in the modern tablet computer with a slim

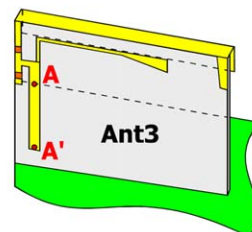
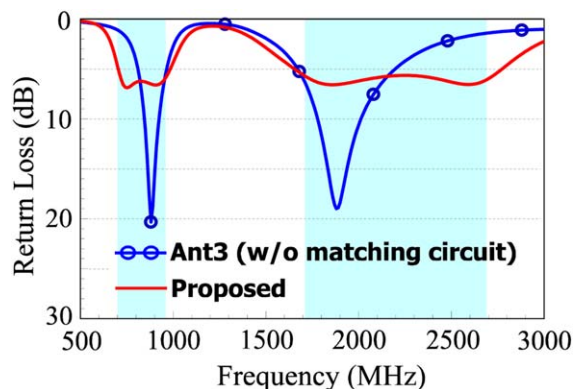
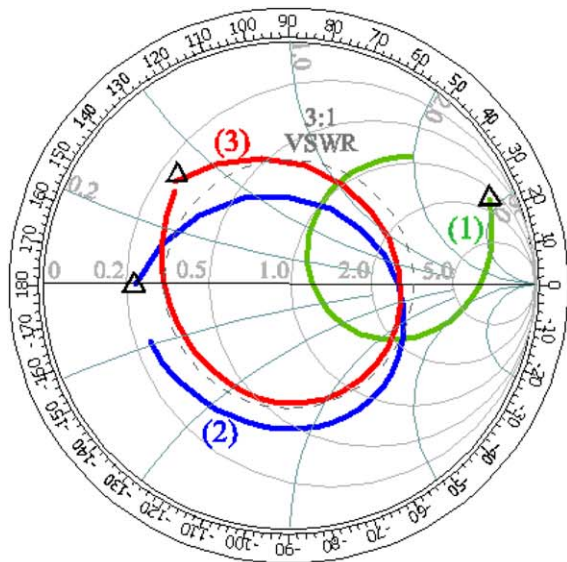
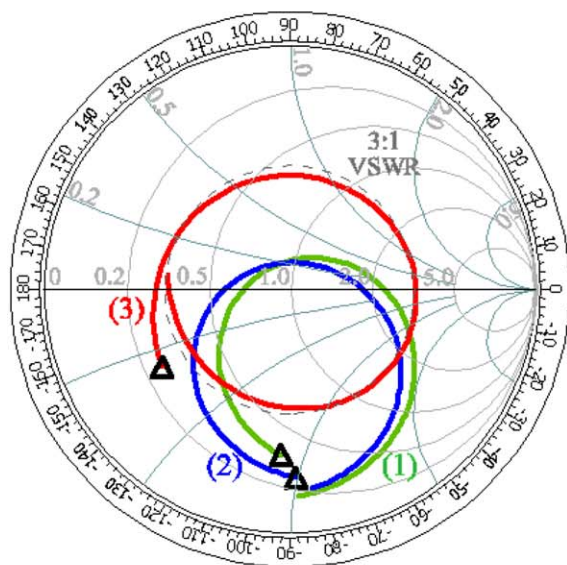


Figure 5 Simulated return loss for the proposed antenna and the case without the matching circuit (Ant3). [Color figure can be viewed in the online issue, which is available at wileyonlinelibrary.com]



(a) Δ :690 MHz



(b) Δ :1600 MHz

Figure 6 Simulated input impedance on the Smith chart for Ant3 (Curve 1), Ant3 with C_1 only (Curve 2), and Ant3 with C_1 , C_2 , L_3 (i.e., the proposed antenna, Curve 3). (a) Frequency range: 690–1000 MHz. (b) Frequency range: 1600–2700 MHz. [Color figure can be viewed in the online issue, which is available at wileyonlinelibrary.com]

profile or thin thickness. Also note that the matching circuit with C_1 , C_2 , and L_3 is disposed above the device ground plane. In practical applications, the matching circuit can be disposed in a very small area, and the occupied area for the matching circuit can generally be negligible [14].

To confirm the above described operating principle of the proposed antenna, Figure 4 shows the simulated return loss for the proposed antenna, Ant1 (the low-band antenna), and Ant2 (the high-band antenna). Simulated results are obtained using the full-wave electromagnetic field simulator HFSS version 14 [26]. Corresponding dimensions of the three antennas are the same. It is seen that the low-band and high-band antennas shown in Figure 3 indeed generate wideband resonant modes in

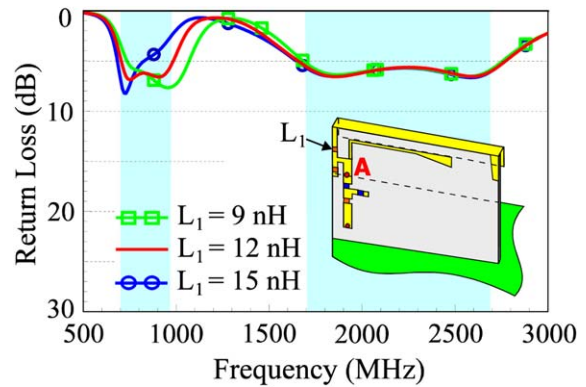


Figure 7 Simulated return loss as a function of the inductance of the chip inductor (L_1). Other parameters are the same as shown in Figure 1. [Color figure can be viewed in the online issue, which is available at wileyonlinelibrary.com]

the desired lower and higher bands (see the two shaded frequency regions in the figure), respectively. Also note that for frequencies in the desired lower and higher bands, the impedance matching of the proposed antenna can have about 6 dB return loss (3:1 VSWR). Although at some frequencies, the impedance matching is slightly less than 6 dB, the obtained antenna efficiency is better than about 50% (see Fig. 11 in Section 4), which is acceptable for practical applications [14]. The related measured results will be discussed in Section 4.

A comparison of the simulated return loss of the proposed antenna with and without the matching circuit (C_1 , C_2 , and L_3) is shown in Figure 5. The case without the matching circuit is denoted as Ant3. It is clearly seen that the matching circuit, respectively, widens the antenna's low-band and high-band bandwidths to cover the desired 698–960 and 1710–2690 MHz bands. As discussed earlier, the low-band bandwidth enhancement is obtained owing to the high-pass matching circuit formed by the capacitor C_1 and the inductor L_2 in the shorting strip. While, the high-band bandwidth enhancement is achieved with the aid of the low-pass matching circuit formed by the capacitor C_2 and inductor L_3 .

Effects of the matching circuit on the bandwidth enhancement are discussed with the aid of Figure 6. In the figure, the simulated input impedance on the Smith chart for Ant3 (Curve 1), Ant3 with C_1 only (Curve 2), and Ant3 with C_1 , C_2 , L_3 (i.e., the proposed antenna, Curve 3) is presented. In Figure 6(a), the frequency range of the simulated input impedance is from 690 to

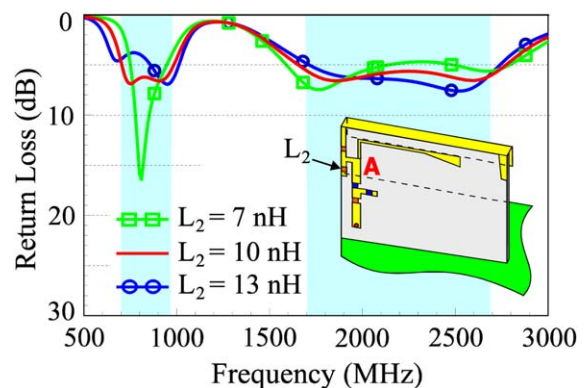


Figure 8 Simulated return loss as a function of the inductance of the chip inductor (L_2). Other parameters are the same as shown in Figure 1. [Color figure can be viewed in the online issue, which is available at wileyonlinelibrary.com]

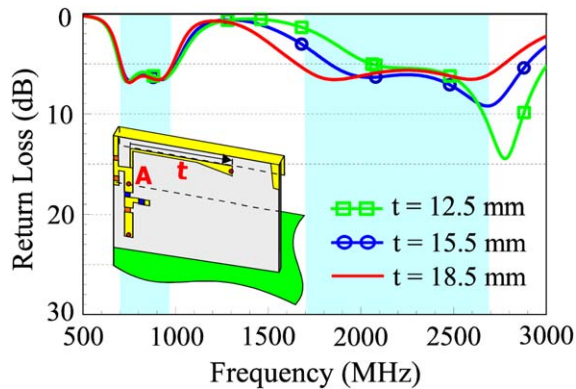


Figure 9 Simulated return loss as a function of the strip length t in the high-band antenna. Other parameters are the same as shown in Figure 1. [Color figure can be viewed in the online issue, which is available at wileyonlinelibrary.com]

1000 MHz, while that in Figure 6(b) is from 1600 to 2700 MHz. In Figure 6(a), by comparing Curve 2 to Curve 1, the impedance curve of the entire desired lower band are shifted within or close to the 3:1 VSWR circle. This behavior, as explained earlier, is attributed to the high-pass matching circuit formed by the capacitor C_1 and the inductor L_2 in the shorting strip. Furthermore, when the elements C_2 and L_3 are added, although they are mainly used to improve the high-band matching, better impedance matching in the entire lower band is also seen (see Curve 2 vs. Curve 3). In Figure 6(b), the adding of C_1 shows slight effects on the high-band impedance matching (see Curve 1 vs. Curve 2). However, when the elements C_2 and L_3 are added, the impedance curve of the entire desired higher band is in general shifted into the 3:1 VSWR circle (see Curve 3 vs. Curve 2). This is mainly because the capacitor C_2 and inductor L_3 formed as a low-pass matching circuit to effectively enhance the high-band bandwidth.

3. PARAMETRIC STUDIES

When the low-band and high-band antennas are formed into the proposed antenna, some parameters such as the inductors (L_1, L_2) in the low-band antenna and the strip length t in the high-band antenna can be used to find-tune the antenna performances. Figure 7 shows the simulated return loss as a function of the inductance of the chip inductor (L_1). Other parameters are the same as shown in Figure 1. Results for $L_1 = 9, 12,$ and 15 nH are presented. It is seen that the high-band operation is almost not affected for L_1 varied from 9 to 15 nH. Conversely, the lower band is shifted to lower frequencies

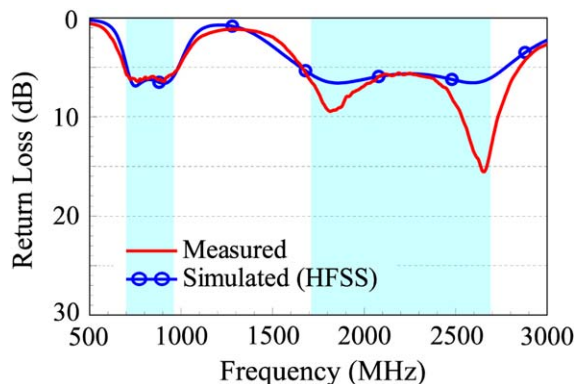


Figure 10 Measured and simulated return losses of the fabricated antenna. [Color figure can be viewed in the online issue, which is available at wileyonlinelibrary.com]

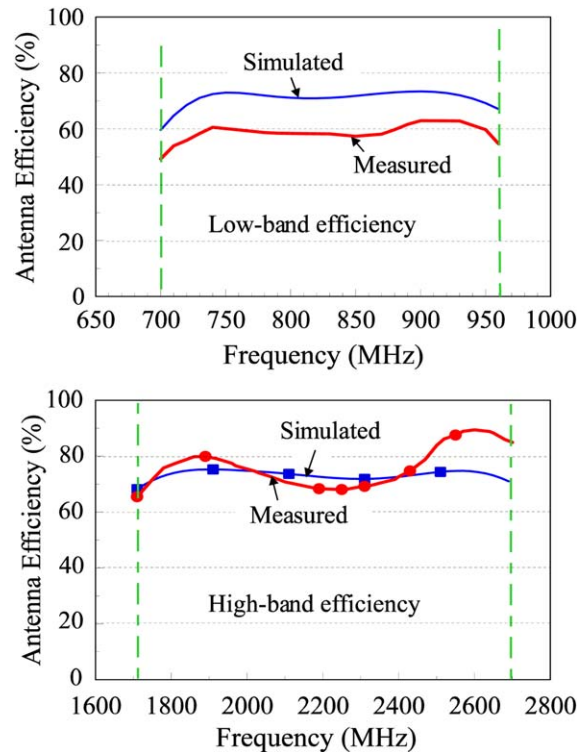


Figure 11 Measured and simulated antenna efficiencies of the fabricated antenna. [Color figure can be viewed in the online issue, which is available at wileyonlinelibrary.com]

with an increased inductance of L_1 . This behavior confirms that the inductor L_1 can decrease the low-band resonant mode and thus can be used to fine adjust the antenna's lower band.

Figure 8 shows the simulated return loss as a function of the inductance of the chip inductor (L_2). Other parameters are the same as shown in Figure 1. For $L_2 = 7$ nH, it is seen that dual-resonance excitation in the lower band is not obtained. Relatively large effects on the high-band performance are also seen. This is mainly because variations in the inductor L_2 will cause variations on the effect of the high-pass matching circuit (L_2, C_1), thus leading to large effects on the impedance matching of the lower band. In addition, when the inductor L_2 has a smaller inductance, the shorting strip will no longer behave like an open circuit at higher frequencies, which causes increased correlation between the low-band and high-band antennas. Hence, a larger inductance for L_2 is preferable in the proposed design. The L_2 is selected to be 10 nH in the proposed antenna. In this case, proper dual-resonance excitation can be obtained for the desired lower band (comparing the results for $L_2 = 10$ and 13 nH).

Figure 9 shows the simulated return loss as a function of the strip length t in the high-band antenna. Other parameters are the same as shown in Figure 1. It is clearly seen that variations in the length t almost not affect the low-band performance of the antenna. This behavior confirms the low correlation of the low-band and high-band antennas in the proposed design. Conversely, with decreasing length of t , the higher band is shifted to higher frequencies. This behavior also suggests that the antenna's higher band can be easily fine-tuned by varying the length t in the high-band antenna.

4. EXPERIMENTAL RESULTS

The fabricated antenna mounted at the top edge of the device ground plane as shown in Figure 2 was tested. A 50- Ω SMA connector is connected to the antenna's feeding port (point A') through a via-hole

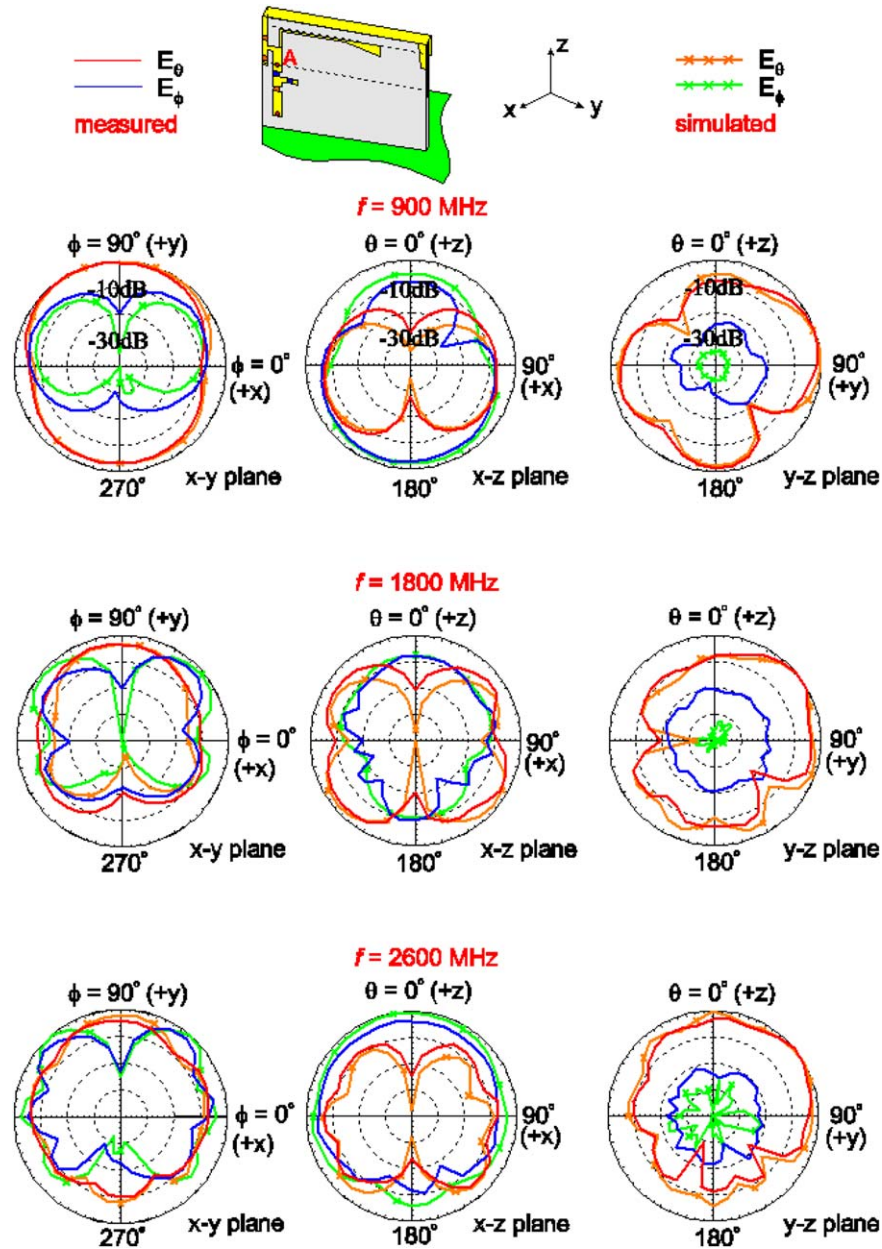


Figure 12 Measured and simulated radiation patterns of the fabricated antenna. [Color figure can be viewed in the online issue, which is available at wileyonlinelibrary.com]

in the FR4 substrate. The antenna is then fed through the SMA connector. The measured and simulated return losses of the fabricated antenna are presented in Figure 10. Agreement between the measured data and simulated results is seen. For frequencies over the lower and higher bands, the measured return loss is better than 6 dB (3:1 VSWR). The measured and simulated antenna efficiencies of the fabricated antenna are shown in Figure 11. The measured antenna efficiency is, respectively, about 50–62% and 66–90% in the lower and higher bands, which are acceptable for practical mobile communication applications [14]. It is also noted that there are discrepancies between the measured and simulated antenna efficiencies, especially in the lower band. This is largely owing to the ohmic loss of the lumped elements in the proposed antenna, especially the chip inductors (L_1 , L_2) in the low-band antenna (see Fig. 3), which is not included in the simulation.

Figure 12 shows the measured and simulated radiation patterns of the fabricated antenna. Results for three representative frequen-

cies of 900, 1800, 2600 MHz are plotted. At each frequency, the radiation patterns in the three principal planes of x - y , x - z , and y - z planes are normalized with respect to the same maximum intensity. Agreement between the measurement and simulation is generally seen. In the x - y plane (azimuthal plane), variations of the E_θ radiation are seen to be much smoother at 900 MHz than at 1800 and 2600 MHz. While in the x - z plane (elevation plane), stronger radiation in the lower half-plane is observed at 900 MHz. On the contrary, stronger radiation in the upper half-plane is observed at 2600 MHz. This behavior is largely because the device ground plane functions more like a radiator at lower frequencies (900 MHz). Conversely, at higher frequencies (1800 and 2600 MHz), the device ground plane functions more like a reflector. In the y - z plane (elevation plane and the plane where the device ground plane is located), the radiation patterns are asymmetric with respect to the z -axis. This behavior is mainly owing to the antenna asymmetrically located along the top edge of the device ground plane.

5. CONCLUSION

A combined-type dual-wideband antenna suitable for 2G/3G/4G tablet device applications has been proposed. The antenna comprises two separate radiation portions and matching circuits and can be decomposed into a low-band antenna (an inverted-F antenna) and a high-band antenna (a monopole antenna) with small correlation. The low-band and high-band antennas can be configured into a compact structure to occupy a small ground clearance of $10 \times 30 \text{ mm}^2$ and a thin thickness of 3 mm. Two wide operating bands of 698–960 and 1710–2690 MHz for the 2G/3G/4G operations can be obtained. Tuning of the lower and higher bands can also be easily controlled by the low-band and high-band antennas in the proposed combined-type antenna. Good radiation performance for frequencies over the two wide operating bands has also been obtained. The proposed combined-type antenna can provide a new antenna design concept with compact size and easy tuning for achieving two wide operating bands for the 2G/3G/4G mobile tablet device application.

REFERENCES

1. K.L. Wong, *Planar Antennas for Wireless Communications*, Wiley, New York, 2003.
2. C.H. Chang and K.L. Wong, Printed $\lambda/8$ -PIFA for penta-band WWAN operation in the mobile phone, *IEEE Trans Antennas Propag* 57 (2009), 1373–1381.
3. D.L. Huang, H.L. Kuo, C.F. Yang, C.L. Liao, and S.T. Lin, Compact multibranch inverted-F antenna to be embedded in a laptop computer for LTE/WWAN/IMT-E Applications, *IEEE Antennas Wirel Propag Lett* 9 (2010), 838–841.
4. S.C. Chen and K.L. Wong, Bandwidth enhancement of coupled-fed on-board printed PIFA using bypass radiating strip for eight-band LTE/GSM/UMTS slim mobile phone, *Microwave Opt Technol Lett* 52 (2010), 2059–2065.
5. C.L. Ku, W.F. Lee, and S.T. Lin, A compact slot inverted-F antenna to be embedded in the laptop computer for LTE/WWAN applications, *Microwave Opt Technol Lett* 53 (2011), 1829–1832.
6. T.W. Kang, K.L. Wong, L.C. Chou, and M.R. Hsu, Coupled-fed shorted monopole with a radiating feed structure for eight-band LTE/WWAN operation in the laptop computer, *IEEE Trans Antennas Propag* 59 (2011), 674–679.
7. S.C. Chen and K.L. Wong, Planar strip monopole with a chip-capacitor-loaded loop radiating feed for LTE/WWAN slim mobile phone, *Microwave Opt Technol Lett* 53 (2011), 952–958.
8. Y.L. Ban, S.C. Sun, J.L.W. Li, and W. Hu, Compact coupled-fed wideband antenna for internal eight-band LTE/WWAN tablet computer applications, *J Electromagn Waves Appl* 26 (2012), 2222–2233.
9. K.L. Wong, H.J. Jiang, and T.W. Weng, Small-size planar LTE/WWAN antenna and antenna array formed by the same for tablet computer application, *Microwave Opt Technol Lett* 55 (2013), 1928–1934.
10. K.L. Wong and T.W. Weng, Small-size triple-wideband LTE/WWAN tablet device antenna, *IEEE Antennas Wirel Propag Lett* 12 (2013), 1516–1519.
11. C.Y.D. Sim and Y.L. Chien, A dual-band coupled-fed LTE/WWAN planar antenna for mobile devices, *Microwave Opt Technol Lett* 55 (2013), 1851–1856.
12. S. Jeon, S. Oh, H.H. Kim, and H. Kim, Mobile handset antenna with double planar inverted-E (PIE) feed structure, *Electron Lett* 48 (2012), 612–614.
13. S. Jeon and H. Kim, Mobile terminal antenna using a planar inverted-E feed structure for enhanced impedance bandwidth, *Microwave Opt Technol Lett* 54 (2012), 2133–2139.
14. K.L. Wong and M.T. Chen, Small-size LTE/WWAN printed loop antenna with an inductively coupled branch strip for bandwidth enhancement in the tablet computer, *IEEE Trans Antennas Propag* 61 (2013), 6144–6151.
15. J.H. Lu and F.C. Tsai, Planar internal LTE/WWAN monopole antenna for tablet computer application, *IEEE Trans Antennas Propag* 61 (2013), 4358–4363.
16. J.H. Lu and Z.W. Lin, Planar compact LTE/WWAN monopole antenna for tablet computer application, *IEEE Trans Antennas Propag Lett* 12 (2013), 147–150.
17. S.H. Chang and W.J. Liao, A broadband LTE/WWAN antenna design for tablet PC, *IEEE Trans Antennas Propag* 60 (2012), 4354–4359.
18. W.S. Chen and W.C. Jhang, A planar WWAN/LTE antenna for portable devices, *IEEE Antennas Wirel Propag Lett* 12 (2013), 19–23.
19. K.L. Wong and T.W. Weng, Coupled-fed shorted strip antenna with an inductively coupled branch strip for low-profile, small-size LTE/WWAN tablet computer antenna, *Microwave Opt Technol Lett* 56 (2014), 1041–1046.
20. K.L. Wong, T.W. Kang, and M.F. Tu, Internal mobile phone antenna array for LTE/WWAN and LTE MIMO operations, *Microwave Opt Technol Lett* 53 (2011), 1569–1573.
21. K.L. Wong, M.F. Tu, C.Y. Wu, and W.Y. Li, On-board 7-band WWAN/LTE antenna with small size and compact integration with nearby ground plane in the mobile phone, *Microwave Opt Technol Lett* 52 (2010), 2847–2853.
22. Y.L. Ban, C.L. Liu, J.L.W. Li, and R. Li, Small-size wideband monopole with distributed inductive strip for seven-band WWAN/LTE mobile phone, *IEEE Antennas Wirel Propag Lett* 12 (2013), 7–10.
23. Y.L. Ban, C.L. Liu, J.L.W. Li, J. Guo, and Y. Kang, Small-size coupled-fed antenna with two printed distributed inductors for seven-band WWAN/LTE mobile handset, *IEEE Trans Antennas Propag* 61 (2013), 5780–5784.
24. K.L. Wong and S.C. Chen, Printed single-strip monopole using a chip inductor for penta-band WWAN operation in the mobile phone, *IEEE Trans Antennas Propag* 58 (2010), 1011–1014.
25. C.H. Chang and K.L. Wong, Small-size printed monopole with a printed distributed inductor for penta-band WWAN mobile phone application, *Microwave Opt Technol Lett* 51 (2009), 2903–2908.
26. Available at <http://www.ansys.com/products/>, ANSYS HFSS.

© 2014 Wiley Periodicals, Inc.

EXPERIMENTAL VERIFICATION OF TUNABLE PROPERTY OF A ZERO-ORDER RESONATOR ON FERRITE SUBSTRATE

Aziza Zermene,^{1,2,3,4,5,6} Bruno Sauviac,^{1,2,3} Bernard Bayard,^{1,2,3} Beatrice Payet-Gervy,^{1,2,3} Jean Jaques Rousseau,^{1,2,3} and Abdelmadjid Benghalia^{4,5}

¹Université de Lyon, F-69000, Lyon, France

²Université de Saint-Etienne, F-42000, Saint-Etienne, France

³Télécom Saint-Etienne, école associée de l'Institut TELECOM, Laboratoire LT2C (Télécom Claude Chappe)

⁴Université Mentouri de Constantine1, Algérie

⁵Laboratoire LHS (Laboratoire des Hyperfréquences et

Semiconducteurs), Route d'Ain EL Bey 25000 Constantine, Algérie

⁶Université Hadj Lakhdar de Batna, Algérie

Received 16 April 2014

ABSTRACT: This article presents a composite right-left-handed (CLRH) zeroth-order resonator designed on a ferrite substrate. Numerical modelling and measurements of the device are presented. The proposed structure is realized in coplanar waveguide configuration using an interdigital capacitor and a shortcircuited stub inductor to add the left-handed property to the resonator. The ferrite substrate is magnetized in a direction perpendicular to the propagation direction. The tunable nature of the proposed device can be achieved by changing the applied magnetic bias. The resonator is designed to be tuned over the 3–5 GHz frequency band. Measured insertion loss is 5 dB giving interesting